Available online at www.sciencedirect.com
SCIENCE DIRECT
Talanta 68 (2006) 1353–1358
Talanta
www.elsevier.com/locate/talanta

ZnS quantum dots derived a reagentless uric acid biosensor

Fenfen Zhang [a], Chenxin Li [a], Xiaohua Li [a], Xiaoli Wang [a], Qiao Wan [a], Yuezhong Xian [a], Litong Jin [a,*], Katsunobu Yamamoto [b]

[a] *Department of Chemistry, East China Normal University, Shanghai 200062, China*
[b] *BAS Co. Ltd., No. 36-4, 1-Chome, Oshiage, Sumida-Ku, Tokyo 131, Japan*

Received 15 March 2005; received in revised form 27 July 2005; accepted 27 July 2005
Available online 15 September 2005

Abstract

A reagentless amperometric uric acid biosensor based on zinc sulfide (ZnS) quantum dots (QDs) was firstly developed. It could detect uric acid without the presence of an electron mediator. The carboxyl group functionalized ZnS QDs were synthesized, and they were soluble biocompatible and conductive. ZnS QDs conjugates could provide increased enzyme binding sites, which may result in higher enzyme loading. Thus, the proposed uricase/ZnS QDs/L-cys biosensor exhibited higher amperometric response compared to the one without QDs (uricase/L-cys biosensor). In addition, there was little AA interference. It showed a linear dependence on the uric acid concentration ranging from 5.0×10^{-6} to 2.0×10^{-3} mol L^{-1} with a detection limit of 2.0×10^{-6} mol L^{-1} at 3σ.

Keywords: Reagentless biosensor; ZnS quantum dots; Uricase; Uric acid

1. Introduction

Uric acid represents the major catabolite of purine breakdown in humans. Therefore, it remains an important marker molecule for disorders associated with alterations of the plasma urate concentration such as hyperuricemia (gout), renal impairment, leukemia, ketoacidosis, Lesch–Nyhan syndrome and lactate excess [1]. Uric acid is also to act as an antioxidant in human body [2]. Consequently its measurement for diagnosis and treatment of some disorders is routinely required [3]. Between the different approaches to accomplish the uric acid determination, such as chemiluminescence method [4], radiochemical–HPLC [5], voltammetric–coulometric [6] and enzymatic–spectrophotometric methods [7], amperometric biosensors have the advantages in less procedures with low cost instrumentation and improved selectivity.

The properties of quantum dots (QDs) result from quantum-size confinement, which occurs when metal and semiconductor particles are smaller than their exciton Bohr radii (about 1–5 nm) [8]. Recent advances have resulted in the large-scale preparation of relatively monodisperse QDs. These QDs are widely used in photocatalysis [9], luminescence [10–15], bioconjugates [16–18] and optical biosensors [19]. Chan and Nie used mercaptoacetic acid for QDs' solubilization and as biological labels [8]. Additionally, Wang demonstrated that by introducing up to three different QDs tags (ZnS, CdS, and PbS), simultaneous DNA assays with 0.3 nM detection limits could easily be electrochemically stripping detection of metal tags [20–22]. However, there is rarely report on the application of QDs in the amperometric biosensor.

Yoneyama et al. immobilized uricase and an electron mediator (MMP) on an Au electrode coated with a biomimetic phospholipids/alkanethiolate bilayer membrane [23]. Kan et al. developed a polyamine-uricase biosensor by template process [24]. Akyilmaz et al. constructed a biosensor based on urate oxidase–peroxidase coupled enzymes system for uric acid determination in urine [25]. The method is relied on generation of H_2O_2 from uric acid by urate oxidase and its consuming by peroxidase and then measurement of the

* Corresponding author. Tel.: +86 21 6223 2627; fax: +86 21 6223 2627.
E-mail address: fenfenzhang@yahoo.com.cn (L.T. Jin).

0039-9140/$ – see front matter © 2005 Elsevier B.V. All rights reserved.
doi:10.1016/j.talanta.2005.07.051

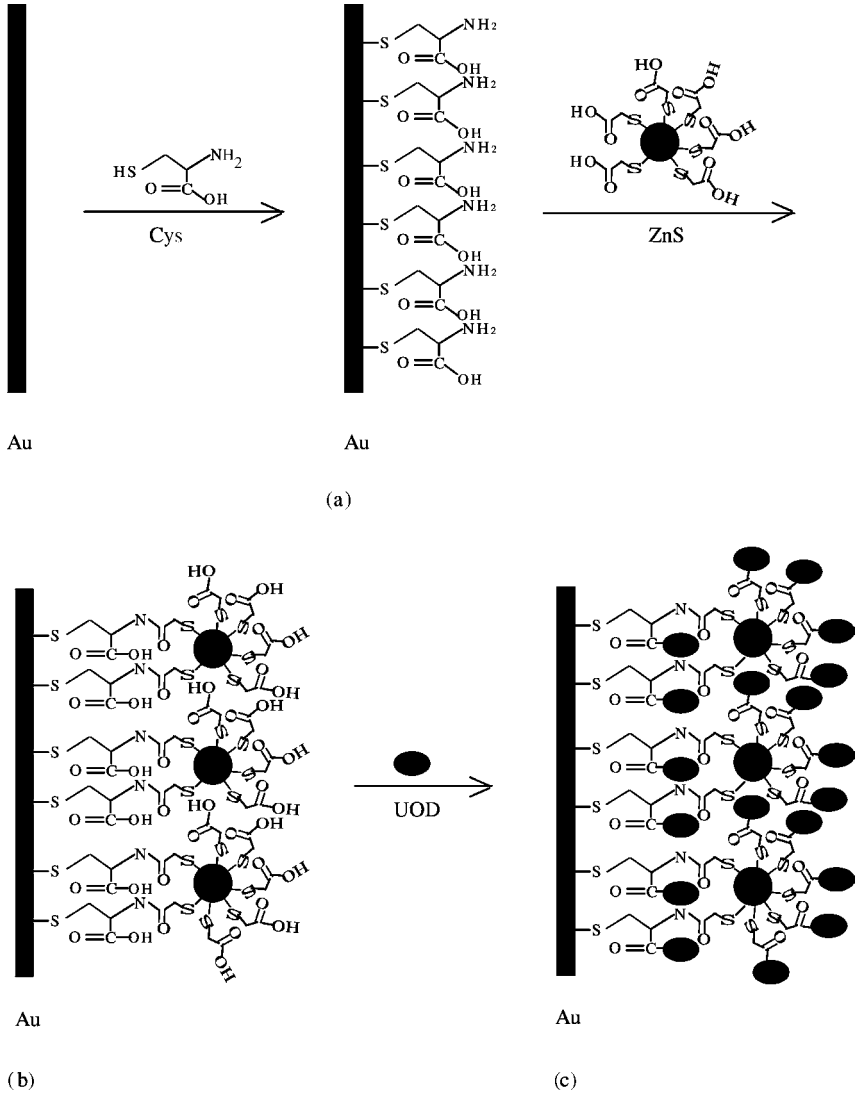

Fig. 1. Schematic representation of the steps to develop a uricase/ZnS QDs/L-cysteamine sensor.

decreasing of dissolved oxygen concentration by the biosensor. However, its linear range was narrow (between 0.1 and 0.5 μm).

In this context, a kind of ZnS QDs with free carboxyl groups on its surface was synthesized in aqueous solution. These nanometer-sized conjugates were water-soluble and biocompatible [8]. ZnS is a semiconductor in terms of relatively large band-gap energy of 3.66 eV and good conductivity [9]. The free carboxyl group is available for covalent coupling to uricase by cross-linking to reactive amine groups [8]. Fig. 1 outlines the steps of developing a reagentless uric acid biosensor, including self-assembly L-cysteamine on Au electrode (a), the carboxyl group functionalized ZnS QDs covalent attached on the L-cys SAM (b), and finally in the presence of EDC, uricase cross-linking on them (c). This work immobilizes directly uricase to a short ZnS QDs/L-cysteamine chain at the gold electrode. The small-sized ZnS QDs can provide more binding sites than the non-ZnS QDs modified biosensor. The performance of this proposed uricase/ZnS QDs/L-cys biosensor showed excellent features of sensitivity, biocompatibility, thermal stability, and anti-interference.

2. Experimental

2.1. Apparatus

Electrochemical experiments with a CHI 1030 workstation (CH instruments, Inc.) were performed at room temperature in a conventional three-electrode system with gold disk working electrode (BAS Co.), platinum wire as the auxiliary electrode, and the saturated calomel as reference electrode. All the differential pulse voltammetry (DPV) parameters were as following: increase potential (0.004 V), amplitude (0.05 V), pulse width (0.05 V), sam-

pling width (0.0167 s), pulse period (0.2 V) and quite time (2 s).

TEM image was recorded by a JEOL JSM-6700F Electron Microscope (Japan).

2.2. Reagents

Uricase (EC 1.7.3.3, 25 units/1.5 mg, from *Arthrobacter gloiformis*), uric acid (purity was +99%), β-D-glucose, 1-ethyl-3-(3-dimethylaminopropyl) carbodiimide (EDC), mercaptoacetic acid (RSH) were purchased from Sigma Chemical Co. Other reagents were commercially available and were of at least analytical-reagent grade. All solutions were prepared using doubly distilled water.

2.3. Preparation of ZnS quantum dots

All glassware used in the following procedures was cleaned in a bath of freshly prepared 3:1 HCl–HNO_3, rinsed thoroughly in distilled water and dried in air. Zinc sulfide quantum dots with free carboxyl groups on its surface were prepared according to the literature [26–28]. Briefly, 38.4 mL mercaptoacetic acid (RSH) was added to 50 mL of 5 mmol L^{-1} $Zn(NO_3)_2$ solution under vigorous stirring, pH was adjusted to 8 with 0.5 mol L^{-1} NaOH and the solution was bubbled with nitrogen for 30 min, then 50 mL of 6.7 mmol L^{-1} Na_2S was dropwise added to the solution. The reaction was carried out for 24 h under nitrogen bubbling. The colloid was stable for weeks at room temperature.

2.4. Construction of uricase/ZnS QDs/L-cysteamine sensor

A gold disk electrode was subjected to the following pretreatment procedures. It was polished with 0.3 μm α-Al_2O_3 and washed ultrasonically with water and absolute ethanol. Before chemical modification, the bare electrode was cleaned in 0.5 M H_2SO_4 by potential scanning between −0.3 and 1.5 V until a reproducible cyclic voltammogram (CV) was obtained. The true area of this gold electrode was about 0.025 cm^2, determined by integration of the cathodic peak for the reduction of the oxide layer. After cleaning, the electrode was rinsed with deionized water and ethanol, and immediately immersed into 0.02 mol L^{-1} L-cysteamine solution for about 24 h at room temperature in the darkness. The resulting monolayer-modified electrode was thoroughly rinsed with water to remove physically adsorbed cysteamine. Then, it was immersed in 100 mL of 0.1 mol L^{-1} EDC and 5.0 mL of ZnS QDs (pH 6.9) for about 2 h, and then rinsed carefully and thoroughly with PBS. Finally, the ZnS QDs modified electrode was incubated in 5 units/mL uricase solutions for 12 h to attach enzyme molecules to the electrode surface. To remove the loosely bound enzyme, the film electrodes were soaked in a pH 6.9 phosphate buffer solution for 5 h before their first use. The sensors were stored at 4 °C when not in use.

2.5. Blood serum samples

Blood serum samples were obtained from volunteers. It was filtered firstly and followed by dilution (1:10) in phosphate buffer solution (pH 6.9) before use. The samples were kept at 4 °C before analysis.

3. Results and discussion

3.1. TEM characterization of ZnS quantum dots

Transmission electron microscopy (TEM) characterized that ZnS QDs did not result in aggregation and were primarily single particles with an average diameter of 4 nm.

3.2. Electrochemistry behavior of uricase/ZnS QDs with a L-cysteamine monolayer-modified gold electrode biosensor

Fig. 2 shows the typical cyclic voltammograms of uricase/ZnS QDS/L-cys/Au in PBS (pH 6.9) (a); in PBS (pH 6.9) contained 5.0×10^{-4} mol L^{-1} uric acid solution (b) and (c) is the control CV of uricase/L-cys/Au in 5.0×10^{-4} mol L^{-1} uric acid solution. Comparing the three voltammograms, a remarkable electrocatalytic oxidation of uricase/ZnS QDS/L-cys/Au was observed. The peak potential (0.381 V) for uric acid of uricase/ZnS QDS/L-cys/Au lowered 169 mV than that (0.550 V) of uricase/L-cys/Au. Furthermore, the peak current of uricase/ZnS QDS/L-cys sensor reached to 3.58×10^{-4} A cm^{-2} mM^{-1}. As uric acid has a background amperometric response at ZnS QDs/L-cys/Au, after cali-

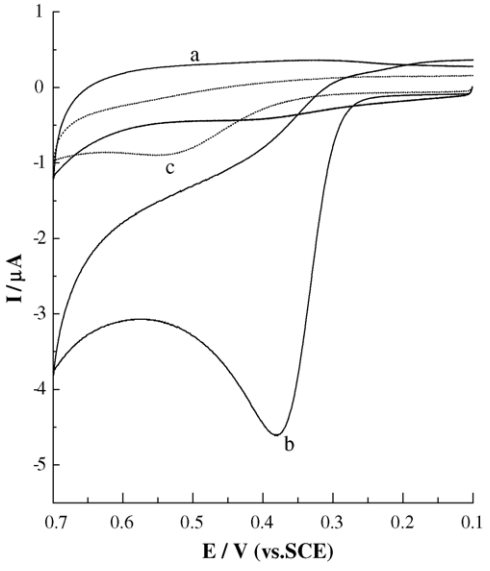

Fig. 2. Cyclic voltammograms of uricase/ZnS QDS/L-cys/Au in PBS (pH 6.9) (a), and in PBS (pH 6.9) contained 5.0×10^{-4} mol L^{-1} uric acid solution (b); uricase/L-cys/Au in PBS (pH 6.9) contained 5.0×10^{-4} mol L^{-1} uric acid solution (c), scan rate: 100 mV s^{-1}.

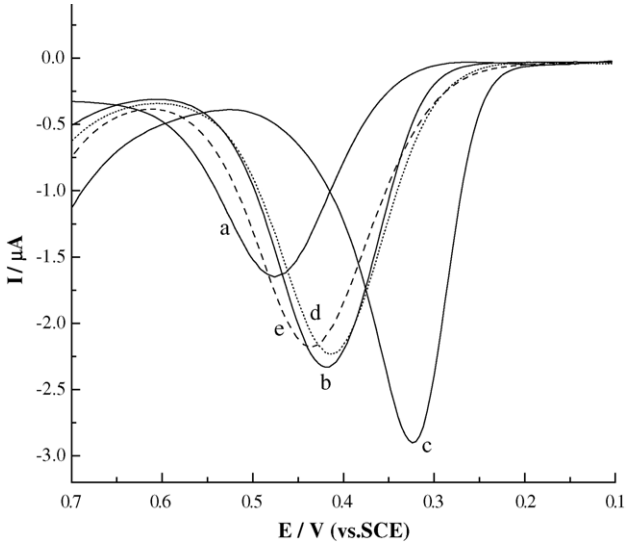

Fig. 3. The effect of pH on the uricase/ZnS QDS/L-cys/Au in PBS containing 5.0×10^{-4} mol L^{-1} uric acid: (a) pH 5.0; (b) pH 6.0; (c) pH 6.9; (d) pH 8.0; (e) pH 9.0.

brated, the peak current was 3.42×10^{-4} A cm^{-2} mM^{-1} and about 7.25 times than that (4.72×10^{-5} A cm^{-2} mM^{-1}) obtained from uricase/L-cys/Au. It may be attributed to higher uricase loading attached on the carboxyl group functionalized ZnS QDs. Additionally, ZnS QDs were highly conductive and biocompatible.

In addition, the peak current versus the square of root of sweep rate plot was linear from 10 to 300 mV s^{-1} (not shown here), indicating that this was a surface diffusion controlled process.

3.3. Effect of pH on the uricase/ZnS QDs/L-cysteamine biosensor

The pH affects the activity of uricase. The pH dependence of the sensor response was evaluated at 5.0×10^{-4} mol L^{-1} uric acid solution over the pH range from 5.0 to 9.0. The amperometric response and the peak potential for uric acid oxidation were changed under the different pH values (Fig. 3). The sensor displayed an optimum sensitivity of response between pH 6.5 and 7.0, which is in good agreement with that reported for soluble uricase. Thus, the ZnS QDs did not change the optimal pH value for the biocatalytic reaction of immobilized uricase to uric acid. Consider the in vivo condition of human body, pH 6.9 was selected for this experiment.

3.4. Thermal stability of the uricase/ZnS QDs/L-cysteamine biosensor

Enzymes or proteins are susceptible to thermal denaturation, however, when they are immobilized onto the conducting surface, their thermal behavior will differ from that they are in the "free" state [29]. Thermal stability is a measure of the practical features of the biosensor to withstand elevations

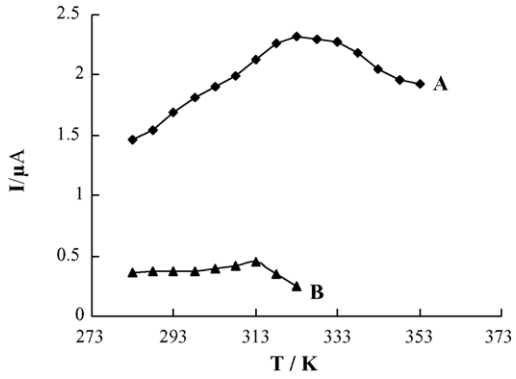

Fig. 4. Relationship between temperature value and response current of the uricase/ZnS QDS/L-cys/Au (A) and uricase/ L-cys/Au (B) in PBS containing 5.0×10^{-4} mol L^{-1} uric acid.

in temperature, frequently in excess of those that normally denature the native enzyme [30,31]. The thermal stability of the uricase/ZnS QDs/L-cysteamine biosensor had been investigated between 283 and 353 K. The DPV responses continued to increase via the increasing of temperatures, which reached a maximum value at 328 K (Fig. 4). Probably, this was due to the activity of uricase enhanced with the increasing of temperatures. However, any further increase of temperature led to a decrease of the sensitivity of the biosensor, which probably was due to the partial denaturation of L-cysteamine or uricase. In contrast, the effect of temperature on the uricase/L-cysteamine biosensor had been investigated under the same condition. The uricase almost lost its activity at 323 K, and showed no DPV response. Therefore, the excellent thermo resistance of the uricase/ZnS QDs/L-cysteamine sensor was probably ascribed to the high conductivity [21] of ZnS QDs and the favorable microenvironment for the binding uricase. Taking both the lifetime and response characteristics into consideration, 298 K was selected in the following work.

3.5. Amperometric response for the uricase/ZnS QDs/L-cysteamine biosensor

Fig. 5(A) shows the DPV response of the sensor to successive increments (1.0×10^{-4} mol L^{-1}) of uric acid solution. These data indicated that the biosensor was in good linear relationship with uric acid concentration. After calibrated from the response of ZnS QDs/L-cysteamine/Au to uric acid, it was linear in the range of 5.0×10^{-6} to 2.0×10^{-3} mol L^{-1} ($r = 0.9996$) (Fig. 5(B, a)). An extremely low detection of 2.0×10^{-6} mol L^{-1} can be estimated at a signal-to-noise ratio of 3.

3.6. Reproducibility and storage stability of the uricase/ZnS QDs/L-cysteamine biosensor

The preparation of the sensor was reproducible. The relative standard deviation of the concentration of a standard

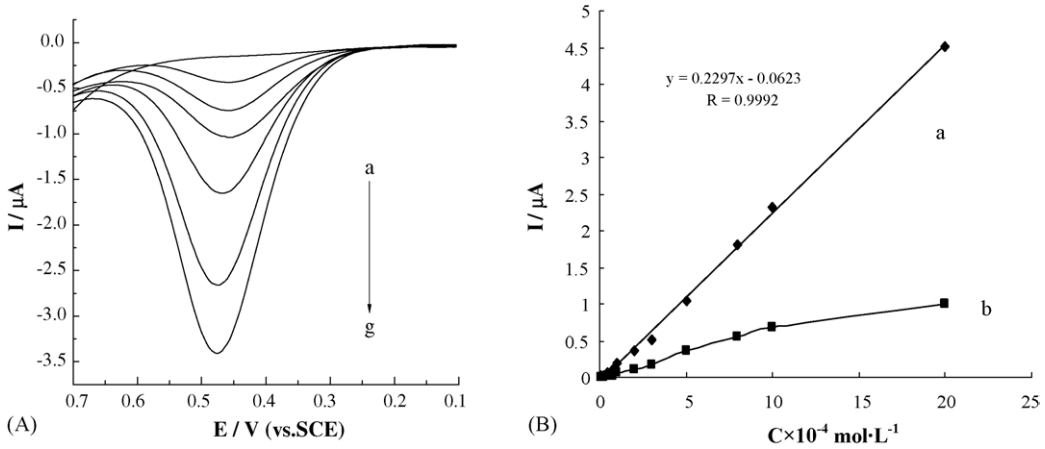

Fig. 5. (A) DPV responses of the uricase/ZnS QDS/L-cys/Au in (a) blank; (b) 1.0×10^{-4} mol L^{-1}; (c) 2.0×10^{-4} mol L^{-1}; (d) 3.0×10^{-4} mol L^{-1}; (e) 5.0×10^{-4} mol L^{-1}; (f) 8.0×10^{-4} mol L^{-1}; (g) 1.0×10^{-3} mol L^{-1} uric acid in PBS (pH 6.9). (B) Linear calibration curve of the uricase/ZnS QDS/L-cys sensor (a) and uricase/L-cys sensor (b).

sample measured with six uric acid sensors, which were prepared under the same conditions, was below 5.3%.

The stabilization action of the sensor was tested in the presence of uric acid (2.0×10^{-4} mol L^{-1}). It lost 4.5% of its initial activity after more than 10 successive measurements. This uric acid sensor had been intermittently used and stored at 4 °C for 20 days, and it maintained 80.5% of its original activity and still displayed an excellent response to uric acid.

3.7. Study on the interference and determination of uric acid in blood samples

Ascorbic acid (AA) and glucose are always co-present with uric acid (UA) in blood samples [32]. The DPV responses of the three analytes were successfully separated by the uricase/ZnS QDs/L-cysteamine biosensor, the oxide peaks of AA and UA were at 0.196 and 0.439 V, respectively, while glucose showed no oxide peak under this condition. Suggesting that, especially at low concentration of uric acid, there was no interference by AA, etc., which might lead to false uric acid measurements.

To test the precision of the uricase/ZnS QDs/L-cysteamine sensor, several assays were made on blood serum samples. The uric acid concentration was determined by the calibration curve and presented in Table 1. Corresponding experiments were carried out with a spectrophotometric method by a local hospital.

As shown in Table 1, the results displayed good consistent and precision between the two methods. However, the sensor method reported in this paper did not require expensive equipment and any other pretreatment of the samples. Therefore, it is possible to obtain a reliable biosensor at very low cost, and the method is useful for application in real samples with good precision and accuracy.

Table 1
Determination of uric acid level in blood samples

Sample number	Determined by spectrophotometry ($\times 10^{-3}$ mol L^{-1})	Measured by biosensor ($\times 10^{-3}$ mol L^{-1})	R.S.D. ($n = 3$) (%)
1[a]	0.50	0.52	1.3
2[a]	0.48	0.49	1.8
3[a]	0.68	0.65	4.4
4	0.35	0.36	3.5
5	0.28	0.26	3.0

[a] The hyper- or hypo-level of uric acid in blood samples, the normal uric acid level in blood is between 0.15 and 0.4 mmol L^{-1}.

4. Conclusion

ZnS QDs with free carboxyl groups on its surface were firstly introduced up to the reagentless amperometric uric acid biosensor. ZnS QDs not only showed good biocompatibility and conductivity, but also functioned as an effective conjugates to provide a sufficient amount of the sites for binding of uricase and L-cysteamine. The ZnS QDs derived uric acid biosensor exhibited high sensitivity, excellent thermal stability, and anti-interference ability.

Acknowledgements

Financial support is acknowledged from the National Natural Science Foundation of China (No. 20327001, 20305007), the Shanghai Nano-Special Foundation (0359nm002) and PhD Program Scholarship Fund of ECNU 2004.

References

[1] J. Woo, D.C. Cannon, in: W.B. Henry (Ed.), Clinical Diagnosis and Management by Laboratory Methods, Saunders, New York, 1991, pp. 140–143.

[2] O. Luz, D. Naidoo, C. Salonikas, Ann. Clin. Biochem. 29 (1992) 674.
[3] E. Miland, A.J.M. Ordieres, P.T. Blanco, M.R. Smyth, C.Ó. Fágáin, Talanta 43 (1996) 785.
[4] M. Tabata, F. Chikaro, O. Matashinge, M. Takashi, J. Appl. Biochem. 6 (1984) 251.
[5] L.G. Michael, S.H. Michael, Anal. Biochem. 176 (1989) 290.
[6] I.F. Abdullin, Y.N. Bakanina, E.N. Turova, G.K. Budnikov, J. Anal. Chem. 56 (5) (2001) 453.
[7] K.B. Ajay, L. Harbans, S.P. Chandra, J. Biochem. Biophys. Meth. 39 (1999) 125.
[8] W.C.W. Chan, S.M. Nie, Science 281 (1998) 2016.
[9] Y. Nakaoka, Y. Nosaka, Langmuir 13 (1997) 708.
[10] M. Jones, J. Nedeljkovic, R.J. Ellingson, A.J. Nozik, G. Rumbles, J. Phys. Chem. B 107 (2003) 11346.
[11] N. Thantu, J. Luminescence 111 (2005) 17.
[12] S.F. Wuister, A. Meijerink, J. Luminescence 105 (2003) 35.
[13] M.J. da Silva, S. Martini, T.E. Lamas, A.A. Quivy, E.C.F. da Silva, J.R. Leite, Microelectron. J. 34 (2003) 631.
[14] Y. Chen, Z. Rosenzweig, Nano Lett. 2 (2002) 1299.
[15] Q. Ma, X.-G. Su, X.-Y. Wang, Y. Wan, C.-L. Wang, B. Yang, Q.-H. Jin, Talanta (2005), http://www.sciencedirect.com.
[16] M. Bruchez, M. Moronne, P. Gin, S. Weiss, A.P. Alivisatos, Science 281 (1998) 2013.
[17] D. Wang, A.L. Rogach, F. Caruso, Nano Lett. 2 (2002) 857.
[18] S.Y. Ding, M. Jones, M.P. Tucker, J.M. Nedeljkovic, J. Wall, M.N. Simon, G. Rumbles, M.E. Himmel, Nano Lett. 3 (2003) 1581.
[19] K.E. Sapsford, I.L. Medintz, J.P. Golden, J.R. Deschamps, H.T. Uyeda, H. Mattoussi, Langmuir 20 (2004) 7720.
[20] E. Bakker, Anal. Chem. 76 (2004) 3285.
[21] J. Wang, D.K. Xu, R. Polsky, J. Am. Chem. Soc. 124 (2002) 4208.
[22] J. Wang, G.D. Liu, G. Rivas, Anal. Chem. 75 (2003) 4667.
[23] T. Nakaminami, S. Ito, S. Kuwabata, H. Yoneyama, Anal. Chem. 71 (1999) 4278.
[24] J. Kan, X. Pan, C. Chen, Biosens. Bioelectron. 19 (2004) 1635.
[25] E. Akyilmaz, M.K. Sezginturk, E. Dinckaya, Talanta 61 (2003) 73.
[26] N.N. Zhu, A.P. Zhang, P.G. He, Y.Z. Fang, Analyst 128 (2003) 260.
[27] N.N. Zhu, A.P. Zhang, Q.J. Wang, P.G. He, Y.Z. Fang, Electroanalysis 16 (2004) 577.
[28] S. Wageh, L.S. Man, F.T. You, X.X. Rong, J. Luminescence 102/103 (2003) 768.
[29] H.H. Weetall, Anal. Chem. 46 (1974) 602A.
[30] L.D. Bowers, Anal. Chem. 58 (1986) 513A.
[31] J. Wang, J. Liu, G. Cepra, Anal. Chem. 69 (1997) 3124.
[32] G.L. Luque, M.C. Rodrí guez, G.A. Rivas, Talanta 66 (2005) 467.